

# Experimental monitoring of hygrothermal transfers and condensation in an insulated rammed earth wall

Girerd Manon<sup>1</sup>, Plé Olivier<sup>1</sup>, Prime Noemie<sup>1</sup>

<sup>1</sup> Université Savoie Mont-Blanc, CNRS, UMR 5271, LOCIE, 73370 Le Bourget du Lac, France

## RESUME

Rammed earth (RE) regulates heat and water vapor according to daily and seasonal cycles, but its high thermal conductivity remains a handicap. To make it a regulatory panel, it is necessary to insulate it. The insulation must guarantee the water balance of the RE to keep its integrity. The use of bio-geo-sourced insulation is relevant especially when contributing to the carbon neutrality of the complex. At the same time, the hygroscopic and capillary properties of these insulations may influence the condensation phenomena and the transfers of water and vapor at the interfaces. To verify this, several conventional and bio-sourced insulations (glass wool, wood fiber, lightweight earth), having the same thermal resistance but distinct hygroscopic and capillary characteristics, associated with a RE wall element are tested. A climatic chamber regulating temperature and humidity on one side of the complex is specifically built while the other side is subjected to stable climatic conditions. A measuring chain monitors the relative humidity, water content, temperature and heat flow through the complex. Different scenarios are applied in order to study hygrothermal transfers and evaluate the conditions for the appearance of condensation at the interfaces. The results of this study should make it possible to establish regulations for the insulation of RE.

**Keywords:** Rammed earth (RE), bio-geo sourced insulation, interface, hygrothermal coupling

## NOMENCLATURE

Symbol	Unit	Definition
$\lambda$	$W.m^{-1}.K^{-1}$	Thermal conductivity
$C_p$	$J.kg^{-1}.K^{-1}$	Specific heat capacity
$\alpha$	$mm^2.s^{-1}$	Thermal diffusivity
$\mu$	-	Water vapor resistance factor
$P_{sat}$	Pa	Saturation vapor pressure
$P_v$	Pa	Partial vapor pressure
RH	%	Relative humidity
$\rho_s$	$kg.m^{-3}$	Dry density
$\rho_w$	$kg.m^{-3}$	Density of water
W	kg/kg	Gravimetric water content
$\epsilon$	F (farads)/m	Absolute dielectric permittivity
$\epsilon_0$	F (farads)/m	Free space dielectric permittivity
$K_a$	[-]	Relative dielectric permittivity; $K_a = \epsilon / \epsilon_0$
$\Theta_v$	$m^3/m^3$	Volumetric water content
Q	$W/m^2$	Heat flux
$W_{80}$	$kg/m^3$	Water content at 80% of relative humidity
A	$kg/m^2.s^{-1/2}$	Liquid water absorption coefficient
VBS	g	Methylene blue value
$W_{80}$	$kg/m^3$	Water content at 80% of relative humidity

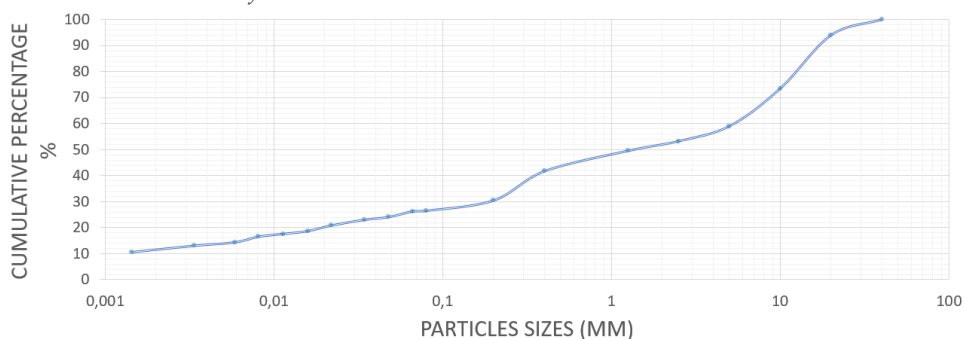
## I. INTRODUCTION

The construction sector is one of the most environmentally impactful [Ahmed Ali et al. 2020]. More specifically, 12% of greenhouse gas emissions in the world are linked to the production of hydraulic binders (cement, plaster, lime). In this context, earth construction – a traditional, ancient, sustainable and renewable technique – which represents 30% of construction in the world, 20% of UNESCO heritage [Gandreau and Joffroy 2013] and 15% of the architectural heritage in France [Fontaine and Anger 2009] offers a potential solution to achieve carbon neutrality objectives by 2050 (Ben-Alon 2021). Earth construction vary by region based on soil, climate, and know-how [Houben et al. 1989]. In Auvergne Rhône Alpes, Rammed Earth (RE) is a traditional technique, involving compacting damp earth between formworks to create load-bearing walls ( $\approx 50$  cm thick). This material, with good thermal inertia, acts as a regulator of daily and seasonal cycles, accumulating or releasing heat and water vapor [Poupard et al. 2024]. However, its high thermal conductivity requires additional insulation to meet current thermal regulations. The choice of insulation is crucial, because of complex hydromechanical coupling of RE [Chauhan et al. 2019]. The insulation must guarantee a balanced water state of the RE material without affecting mechanical behavior. Recent numerical studies by Indekeu [Indekeu 2023] and Giuffrida [Giuffrida et al. 2024] highlight the importance of the hygroscopic and capillary properties of insulation to maintain optimal water balance in insulated RE walls while the water states changes the mechanical properties of the RE walls [Chitimbo et al. 2022]. These publications emphasize the need for experimental validation. To verify this, a climatic chamber is created and a measurement chain developed to monitor temperature, relative humidity and liquid water content in RE insulated complex. Two scenarios were defined to determine firstly the hygrothermal properties of the assemblies and secondly the appearance and evolution of the condensation at the interfaces. After validating the chain of measure by testing scenario on non-insulating RE, three insulating materials assembled with RE, characterized by distinct capillary and hygroscopic properties, will be studied: glass wool, wood fiber and earth-hemp. In this paper the full protocol is presented, with the results of RE wall drying, and first hygrothermal scenario apply on non-insulated RE in the climatic chamber to validate the chain of measure and characterize the hygrothermal behavior of RE.

## II. MATERIALS DESCRIPTION

### A. Rammed earth (RE)

#### 1. Geotechnical classification



[2022]FIGURE 1. Granulometric curve

The earth comes from the north of Isere, France. The granulometric curve, established by sieving (XP P94-041) and sedimentation (NF P94-057) (fig. 1), shows a  $D_{max}$  of 4 cm, 26% of fine grains ( $<80\mu\text{m}$ ), 12% of clay ( $<0.002\text{mm}$ ), and 50% passing at 2mm sieve. The grain size distribution is wide (uniformity coefficient ;  $C_u > 3000$ ) which is characteristic of RE [Houben et al. 1989] and not well graded ( $C_c=5$ ). The clay gives the soil a water retention capacity that plays a crucial role in the cohesion of the material. To assess this clay activity, methylene blue tests (NF P94-068) and Atterberg limits (NF EN ISO 17892-12) were carried out. The VBS value of 1.54 g (measured on the entire soil fraction), is in favor of an “active” clay fraction of soil. The liquid limit (LL) is 28.8% and the plastic limit (PL) is 16.4%, which is consistent with values found in the literature for RE, ranging from 15-46% for LL and 8-26% for PL [Fabbri et al. 2022] . Consequently, the plasticity index is  $IP = 12.4\%$ , which allows the soil to be classified as B6 according to the GTR classification, based on the Atterberg limits, VBS value, and particle size distribution curve.

## 2. *Hygrothermal characterization of the soil*

Thermal conductivity, capacity, and diffusivity were measured using a Hot Disk®, a rapid method suitable for hygroscopic materials, thus minimizing humidity variations during testing [Losini et al. 2023]. Two cylindrical RE samples (15 cm in diameter, 6 cm in height), were prepared according to a strict protocol to ensure reproducibility, with a dry density of  $2015 \pm 27 \text{ kg/m}^3$ . On these samples, two planar zones were selected and marked to perform the Hot Disk® measurements, with the probe positioned between them, ensuring comparable and reproducible results. After a day of drying, the samples were wrapped in cellophane, allowing measurements to be taken one week later, with a water content of 8%. Dry thermal conductivity was determined after drying at  $60^\circ\text{C}$  until mass stabilization (ISO 12571:2013) and storage during two days in airtight boxes with silica gel at 5% relative humidity. Each measurement was repeated five times, the mean value and standard deviation obtained are presented in Table 1. The standard Hot Disk module used in this study give robust result for thermal conductivity while the measurement of the thermal diffusivity values (and, by extension, the heat capacity, which is calculated from these diffusivity value) should be interpreted with caution. Indeed, the thermal diffusivity is measured on a radial plane and is highly sensitive to heterogeneity within the material surface, making the measurement less robust. In particular, the specific heat capacity results do not appear to follow the law of mixtures, which is unexpected and may be attributed to limitations in measurement accuracy. To improve the reliability of these results, additional tests using specific heat capacity module, which allows direct measurement of specific heat capacity rather than calculating, will be conducted in a second time.

The influence of water content on thermal conductivity and specific heat capacity values is highlighted in Table 1. The results show that RE has a high thermal capacity and low thermal diffusivity (Table 1), which helps maintain a relatively stable indoor temperature and promotes good thermal comfort, especially in summer. Unfortunately, its high thermal conductivity (Table 1) requires the addition of insulation in winter to comply with current regulations. Its low resistance to water vapor diffusion around 5.7-20.5 [Chabriac 2014] [Giada et al. 2019] [Chehade et al. 2024] [Losini et al. 2023]) and its ability to adsorb and desorb moisture content makes it an effective regulator of indoor humidity [Poupard et al. 2024]. Indeed, the water content in RE for

RH of 80% and temperature of 21°C, is ranging between 22 and 77 kg/m<sup>3</sup> according to the different RE types [Chehade et al. 2024] [Colinart et al. 2024] [Losini et al. 2023].

**TABLE 1. Hot Disk® results**

Gravimetric water content $W$ kg/kg (%)	8	Dry (=0)
Thermal conductivity $\lambda$ (W.m <sup>-1</sup> . K <sup>-1</sup> )	2.62 (±0.05)	1.243 (±0.05)
Temperature $T$ (°C)	21°C	21°C
Specific heat capacity $C_p$ (J.kg. K <sup>-1</sup> )	908.2 (±20)	684.8 (± 20)
Thermal diffusivity $\alpha$ (mm <sup>2</sup> .s <sup>-1</sup> )	1.43 (±0.01)	0.9(±0.025)

### 3. Construction of RE wall

To ensure the homogenization of the water content and particle size, one week before the construction of the wall, the earth was mixed on external platform using a mechanical shovel and cover. The RE wall was built in accordance with the rules of the art by specialists ([TERA et al. 2018]) under a water content between 11% to 12%. A control of the compaction (expanded and compacted height) and the water content is carried out during the construction [Le Tiec et al. 2020]. For each layer: a height of 12 cm of expanded earth is poured between formwork and compacted with a pneumatic hammer (6.5 bar). The resulting layer obtained has a height of 6 cm (Fig. 2). Monitoring the weight of the earth used and its water content allowed to determine the dry density of the walls of 2034 kg/m<sup>3</sup>. Dimensions of the wall (0.6x0.6x0.2m) have been chosen to limit boundary effects when simulating a unidirectional hygrothermal flux. This wall thickness is representative of half actual thickness of RE building.



**FIGURE 2. Construction of RE wall**

### B. Insulation

The chosen reference glass wool insulation comes in the form of rolls with a thickness of 10 cm, a thermal conductivity of 0.04 W/(m.K) and a dry density of 28 kg/m<sup>3</sup>. Its properties classify it as non-hygroscopic with  $W_{80} < 2$  kg/m<sup>3</sup> according to [Héberlé 2013], and non-capillary (low absorption coefficient value ( $A$ )), but permeable to vapor ( $\mu$  between 0 and 2), which differ significantly from RE properties (fig. 3), potentially leading to moisture-related pathologies due to their distinct responses to temperature and humidity. The selected wood fiber comes as semi-rigid panels, 10 cm thick, with a thermal conductivity of 0.038 W/(m.K) and a dry density of 74.45

kg/m<sup>3</sup>. This material can adsorb water vapor and liquid and is permeable to it. Finally, the chosen lightweight earth (earth-hemp) mix, with thermal conductivity around 0.06 W/m.K and characteristics close to those of RE (fig. 3), is hygroscopic, capillary active and vapour-permeable, storing moisture content [Vincelas 2019].

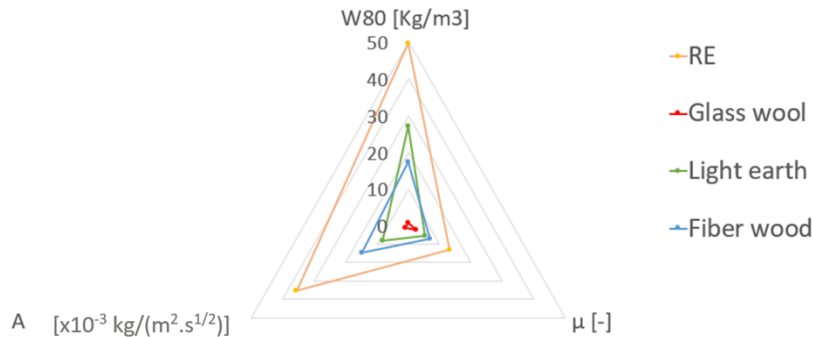


**FIGURE 3.** Average values of hygro-hydro-thermal parameters from the literature review  
 Legend: A = liquid water absorption coefficient, W80 = water content of the material at 80% relative humidity,  $\mu$  = vapor resistance factor.

### III. STUDIES AND SCENARIOS

#### A. PHASE A: RE wall drying

The drying of the RE wall takes place in the uncontrolled conditions of the experimental room. The wall is monitored using three sensors measuring temperature and relative humidity, installed during wall construction in the middle layer: two placed 2 cm inside each face and one at the center of the wall, all protected by hygrometric caps, as done in the study of Chitimbo [Chitimbo 2023]. The drying process is tracked over 300 days, with periodic weight measurements to assess liquid water content. External conditions of the room are also monitored (T, RH).

#### B. PHASE B: Studies RE and assemblies with climatic chamber

##### 1. Scenario 1: Hygrothermal transfers in the hygroscopic domain for RE and insulated RE

This phase imposes a temperature and humidity gradient (coupled transfers) until reach steady state regime during 4 days, to study the complex's response, validating the measurement chain (flowmeter, temperature, relative humidity and water content) and assessing the hygrothermal behavior within the hygroscopic domain of the RE and insulated RE. **A scenario with a 15°C, 50% RH (C<sub>1</sub>) in the room and 12°C, 90% RH (C<sub>2</sub>) in climatic chamber (controlled conditions) will be tested.**

##### 2. Scenario 2: Hygrothermal transfers in the capillary domain; Condensation in insulated RE wall

This phase examines condensation over time under adequate conditions. To determined adequate condition, a sensitivity analysis using the Glaser method (EN ISO 13788) is conducted on a 20cm insulated RE wall. The model is a first approach to assess the condensation risk by considering only water vapor transfer, neglecting moisture storage. Figure 4.a presents the results of this analysis for a RE wall insulated with 10 cm of glass wool. **The applied conditions will include a fixed indoor climate of 20°C/50% RH (C<sub>2</sub>) on the room side, stabilized using a radiator, and 5°C/80% RH (C<sub>1</sub>) on the climatic chamber side, typical for winter in Aura (Poupard et al., 2024).** The Glaser graph shows a condensation zone in grey under these conditions for glass wool insulation (Fig. 4.b). After reaching condensation, the RE wall will be replaced with a dry-one to test a new insulation-RE assembly.

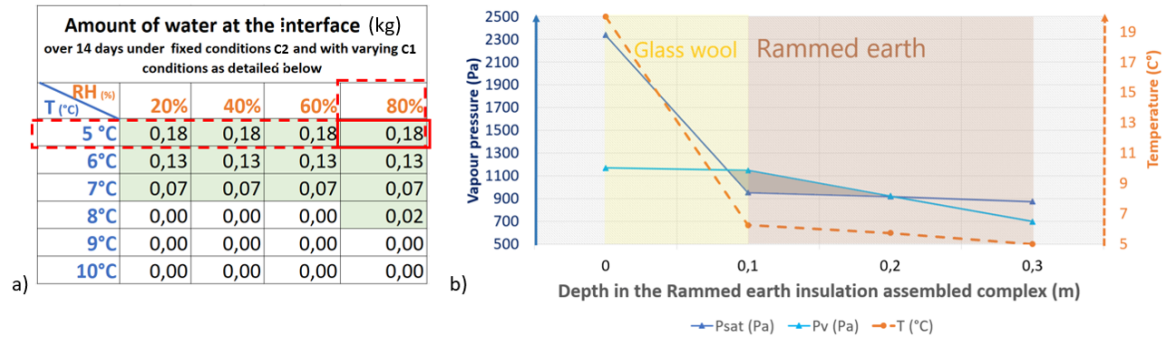


**FIGURE 4.** GLASER for 10 cm Glass wool and 20cm RE, for 0.6x0.6 m wall surface: a) C<sub>2</sub> = 20°C-50%RH / C<sub>1</sub> ranging from 5 to 10°C and 20 to 80% RH, b) C<sub>2</sub> = 20°C-50%RH and C<sub>1</sub> = 5°C,80%RH

### IV. SPECIAL DEVICE AND MEASUREMENT

#### A. Hardware description

A climatic chamber is used to control the temperature and humidity. Using remote probes, this chamber can regulate a remote chamber with a maximum volume of 140l. The dimension of the RE walls are then adapted to fit this remote chamber (Fig. 5). The chamber is insulated with three 10 cm thick PU layers (R<sub>tot</sub> = 13.9 m<sup>2</sup> K/W) assembled to avoid thermal bridges. The weight is measured using Straps and a Kern spring balance (accuracy 0.1kg) with a duct system that can be disconnected from the climatic chamber for weighing. 14 sensirion SHT 75 probes, noticed S1 to S14, were used to measure temperature (±0.4 °C) and humidity (±1.9%), one Campbell CS655, C1, probe measure permittivity, 2 thermocouples, T1 and T2 measure temperature (±1.5 °C), and one square Captec fluxmeter with 5cm sides, F1, monitors heat flux (5 cm, 17.6 μV/(W/m<sup>2</sup>) sensitivity). These probes are connected to Arduino Mega and Campbell CR300 data acquisition systems.

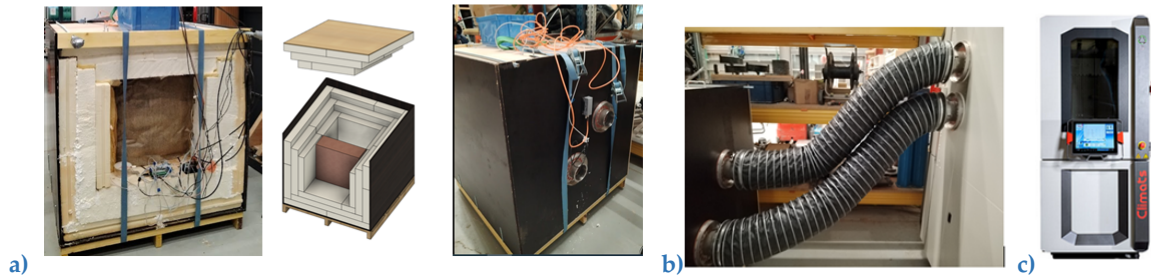


**FIGURE 5.** Remote chamber (a), Connectors (b), climatic chamber (c)

#### B. Sensor's calibration and installation

The CS655 probe was inserted into a hole filled with 4 cm of fine soil (<1.2 mm). This configuration creates an inaccuracy of approximately 10%, as shown by the measurement campaign involving variations in soil cover thickness over the CS655 probe, since the volume investigated by the probe is known to extend up to 7.5 cm around the rods. To improve accuracy, the probe insertion technique should be modified in future experiments to allow for deeper placement into the soil. However, the calibration curved is obtained in lab using same soil and the same configuration (probe placed at 4 cm depth into the soil). The curve (Fig. 6) correlating permittivity (K<sub>a</sub>) (measured by CS655 probe) to volumetric water content (Θ<sub>v</sub> [m<sup>3</sup>/m<sup>3</sup>]) well

follows Topp’s formula (Eq. 1) [Topp et al. 1980]. To obtain the real volumetric water content corrected ( $\Theta_v$ -corrected [ $m^3/m^3$ ]),  $\Theta_v$  is multiplied by the fraction of grains passing through 1.2 mm (50%), assuming larger grains are not hygroscopic, this correction is sometimes proposed [Losini et al. 2023]. Then  $W$  [kg/kg] is calculated using Eq. 2.

$$\theta_v = -5,3 * 10^{-2} + 2.92 * 10^{-2} K_a - 5.5 * 10^{-4} * K_a^2 + 4.3 * 10^{-6} * 3 \tag{1}$$

$$W = \theta_{v-corrected} \frac{\rho_w}{\rho_s} \tag{2}$$

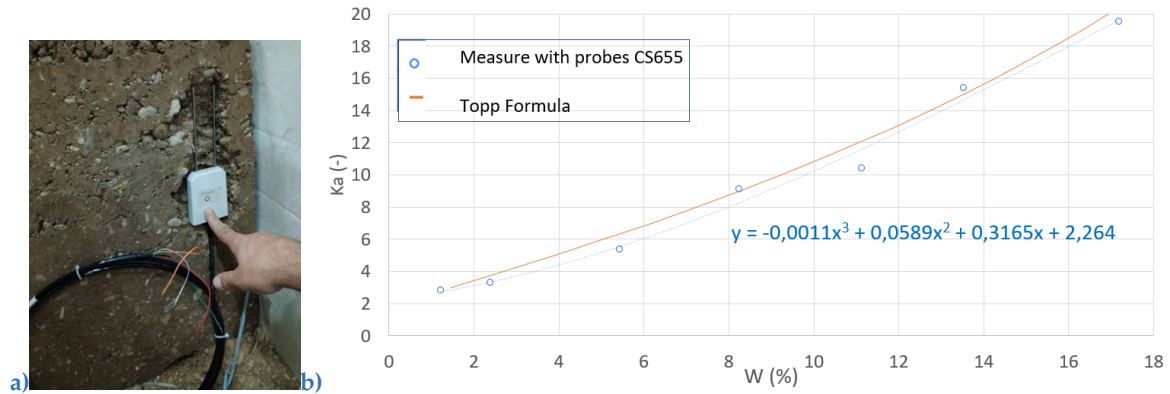


**FIGURE 6.** CS655 introduce on RE (a), Calibration of probes (b)

The SHTs were tested by placing the sensors in a box at 70% RH and 21°C. Sensors with RH  $\pm 1\%$  and T  $\pm 0.5^\circ C$  of the box value were kept. The probes were then positioned in the RE wall during construction (fig 7-a) or incorporated into the insulation.

The Fluxmeter is controlled using a laboratory heating plate that applies a temperature gradient across two polystyrene plates. By knowing the fluxmeter sensitivity (17.6  $\mu V/(W/m^2)$ ), surface area (A), thermal conductivity ( $\lambda$ ), thickness of polystyrene (e) and temperatures (T1-T2), heat flux is calculated using Fourier's law (eq. 3) and compared with fluxmeter reading. The measured flux matches the theoretical value within 0.03W/m2 (0.6% relative error), which is acceptable. The fluxmeter is placed on the surface of the RE wall and secured with an adhesive.

$$Q = \frac{\lambda * A * (T_1 - T_2)}{e} \tag{3}$$

### C. Synthesis of probes positions

The following process of measurement (fig. 7-b) is developed.

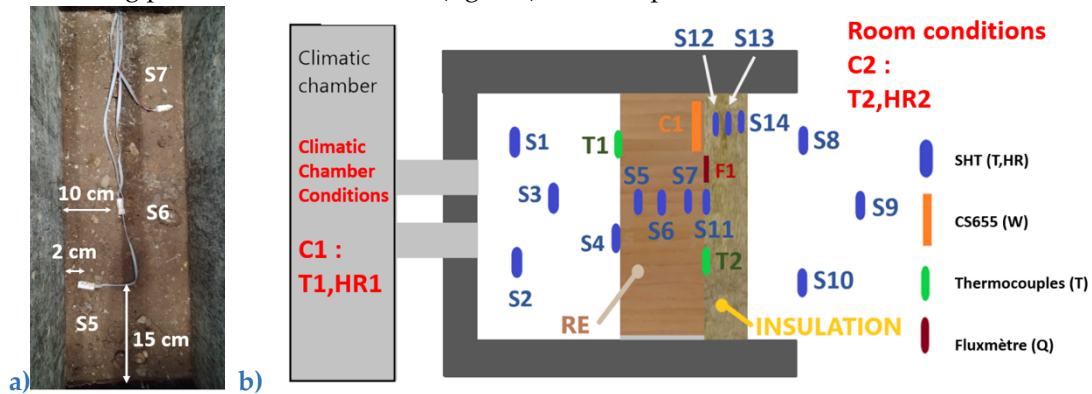


FIGURE 7. Position of probes on the RE wall in top view during the manufacture (a), in a side view (b)

## V. RESULTS AND DISCUSSION

### A. Results of phase A

From March 9, 2024 to January 7, 2025, the drying of the walls was monitored (SHT probes integrated into the walls and ambient conditions), and tracked by weighing. The temperature (T), relative humidity ( $\varphi$ ), water content (W) and vapor pressure (Pv) curves were plotted (Fig. 8). The thermal inertia of RE is highlighted by greater temperature amplitudes in the room than the wall itself (fig 8-c). During the initial drying phase ( $\varphi=100\%$ ), a drop in the temperature of the wall is observed in comparison of room conditions, due to the endothermic process of water evaporation.

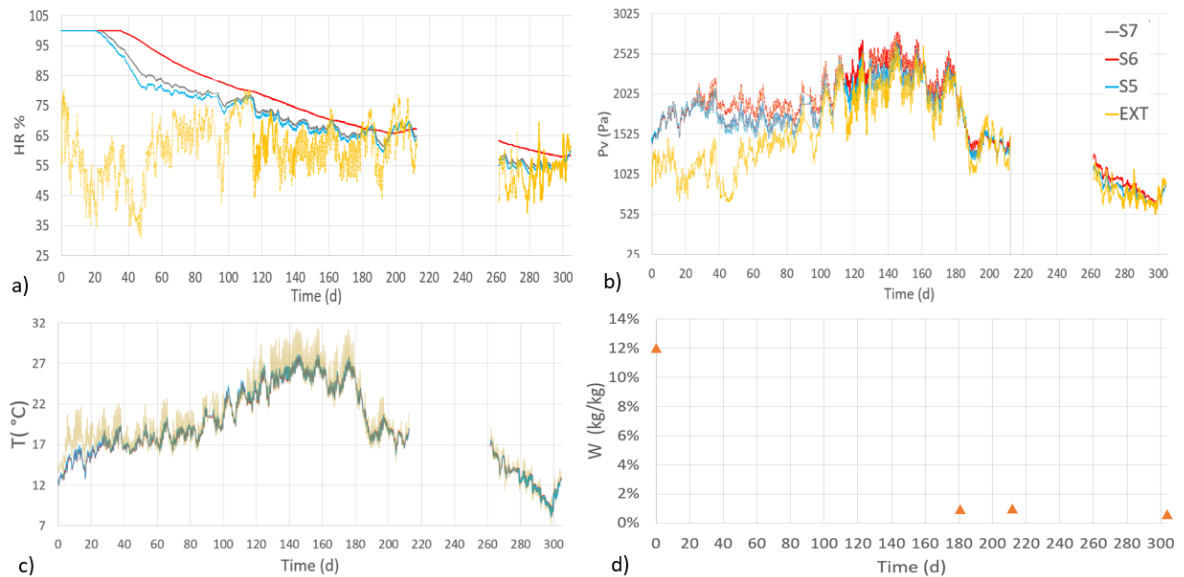
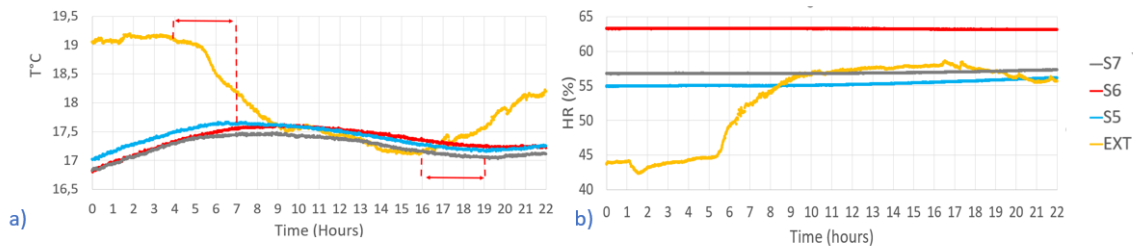


FIGURE 8. Phase A: drying phase;  $\varphi$  (a), Pv (b), T(c), W(d)

Between 100 and 120 days, RH increase in the room induces sorption in the wall, causing temperature increase (exothermic process). As for relative humidity, more marked fluctuations are observed near the surfaces of the wall (2 cm on each side), while humidity remains stable at the core. From 100 days, the vapor pressure follows a similar evolution between the room and the

wall, although remaining higher in the wall. At 200 days, the vapor pressure in the wall becomes equivalent to that of the room, and the gravimetric water content remain stable, marking the end of the drying. In addition, from the 200th day, the temperatures in the wall correspond to the average value of the daily temperature fluctuations in the room, whereas it was generally always lower before which also highlights the end of the endothermic process. These observations indicate that the wall is dry.



**FIGURE 9. Phase A: 24h of drying phase (from 24/11 to 25/11); T [°C] (a), HR (b)**

During a 24-hour drying period, a phase shift of approximately 3 hours is observed between the room temperature and the center of the wall (Fig. 9-a). And despite a relative humidity variation of more than 10% in the room, no significant impact is noticeable on this 24-hour scale on the RE wall even in 2 cm depth.

## B. Results of phase B

### 1. Scenario 1: hygrothermal transfers on uninsulated RE

The test was first conducted on uninsulated RE wall over 4 days. The S3 and T2 sensors did not provide usable results. The temperature and thermal flux data are shown in figure 10-a. Temperature control in the chamber was kept equal to 5°C within  $\pm 1^\circ\text{C}$ , but large temperature variations (between 12 to 16 °C) were observed on the room. Between 12 and 25 hours (fig. 10- a), RE reduced the thermal peak by half compared to the thermal peak on the room. A 6-hour phase shift was observed between the room and the sensor S5 (18cm into the RE). Stable temperature and flux condition are found between 39-50 hours, as shown in figure 10-a, with linear temperature profiles, which allows the application of Fourier's law for the calculation of thermal conductivity. During this period, thermal conductivity values can be computed using Fourier's law (eq. 3) and is found equal to 0.8 W/m.K, i.e. lower than those measured with the hot disk method (1.2 W/m.K for dry RE), likely due to disturbances from radiation and convection, and imperfect contact between the wall and the sensor. There is a vapor pressure gradient in the complex (fig. 10-b), indicating coupled hygrothermal transfers. Vapor pressure increases in the room between 69-87 hours, but the effect was only noticeable on sensors near to the surface S7 (2cm inside RE). Vapor pressure in the middle of the wall remained stable. The C1 sensor showed slight variations on water content, likely related to a humidity peak in the indoor platform (Fig. 10-c).

2. Perspectives to ameliorate the measure

To guarantee stable conditions in the room side, a radiator will be installed to stabilize the climate at 20°C and 50%RH for the following studies on phase 2. Besides, during the next campaign, a thermal paste will be introduced between fluxmeter and the wall to improve the contact. Finally, an anemometer will be put on the climatic chamber to verify the boundary conditions.

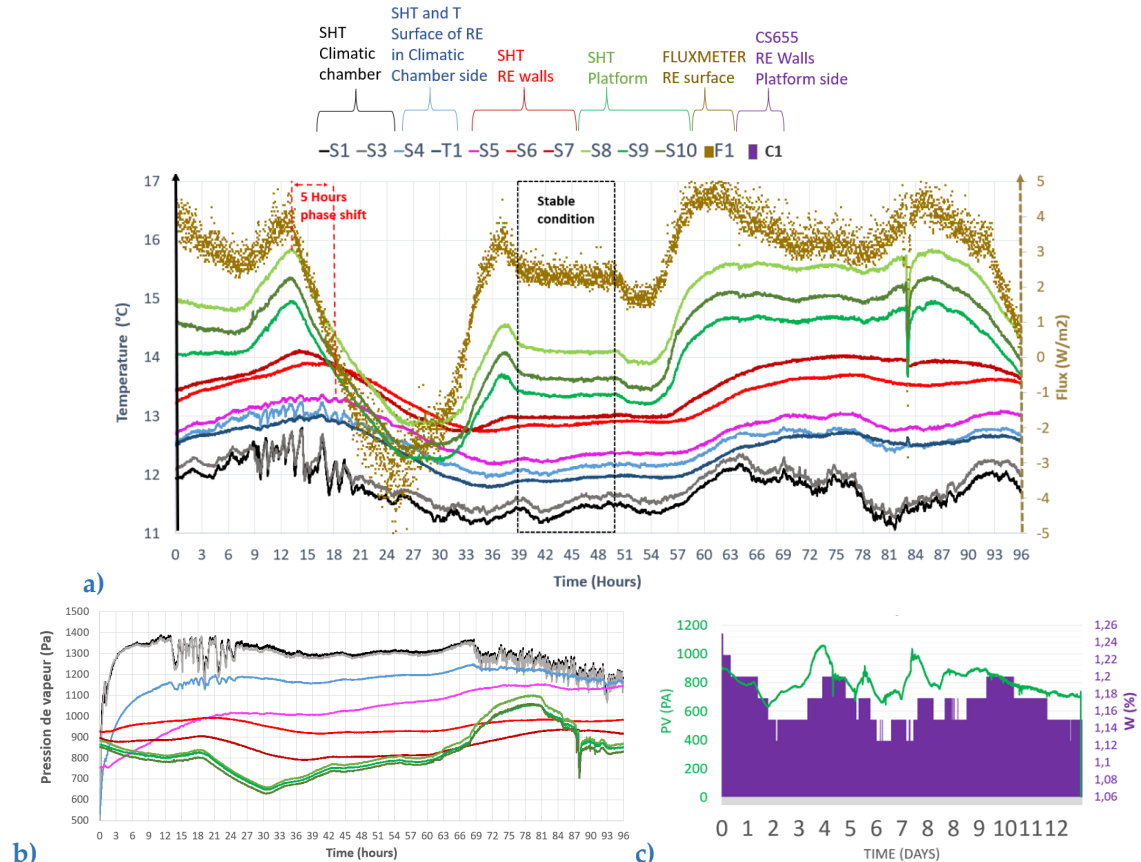


FIGURE 10. Scenario 1 apply on uninsulated RE; Temperature and fluxmeter (a), Vapour pressure (b), Gravimetric water content (c)

## CONCLUSION

The question of insulating RE walls is crucial, where moisture balance is a key to maintain mechanical strength and durability. The main risks associated with insulation include the potential for condensation within the wall assembly and the hindrance of drying processes (water from capillary rise or internal condensation) if water is trapped due to intrinsic properties of materials. Insulation also affects heat and moisture transfers within the wall. A literature review suggests that some insulation materials exhibit hygro-hydro properties more similar to those of RE (cf fig. 3), which could minimize disturbance caused by insulation addition. To assess this, three different assemblies will be test (RE – glass wool, light earth and fiber wood), studied in the hygroscopic domain (cf scenario 1) and in the capillary domain where condensation appears at the interface (cf. scenario 2 as it's explained in part II.B.2). RE wall were built using locally sourced earth by a skilled mason. A test chamber linked to a climate generator, was built to control temperature and humidity and a chain of measure was developed. To validate measure of SHT probes the drying phase of RE was studied. Then, to validate the measurement chain scenario 1 were applied to non-insulated RE. Initial drying analysis revealed: a 3-hour phase shift for 10 cm of RE depth, 200 days required for thorough drying of a 0.6x0.6x0.2 m RE wall, an hygrothermal coupling effect on the drying phase with temperature variation depending on the drying (desorption) or sorption phase. The hygrothermal transfer analysis (scenario 1) in uninsulated RE showed : a 5-hour phase shift for 18 cm of RE depth, halved temperature amplitude within the wall compared to the external environment, water content variations aligned with vapor pressure fluctuations matching the sorption curve (W between 1.14-1.26% at 50-60%RH and 13-14°C), and conductivity data around 0.8 W/ (m.K) for RE. Initial results from non-insulated RE confirmed the reliability of the measurements of temperature, relative humidity and water content data, and the deduction of vapor pressure and conductivity by calculation. The SHT acquisition validity is confirmed by the coherent phase shift in temperature and variations during absorption/desorption and thermal amplitude attenuation. The CS655 acquisition validity is demonstrated by consistent water content data derived from permittivity measurements, and by the variation in water content according to environmental humidity. However, improvements are needed for the flowmeter measurements. Enhancing fluxmeter contact by adding thermal paste should improve result reliability, and positioning the fluxmeter at the interface of RE and insulation, will reduce external disturbances. In summary, the measurement chain is nearly fully validated, with some adjustments needed. Having studied the hygroscopic behavior of non-insulated RE, future research will focus on evaluating the impact of different insulation materials on hygrothermal transfers (scenario 1) and further investigating condensation behavior at the interface within wall assemblies (scenario 2).

## REFERENCES

- AHMED ALI, K., AHMAD, M.I., AND YUSUP, Y. 2020. Issues, Impacts, and Mitigations of Carbon Dioxide Emissions in the Building Sector. *Sustainability*.
- CHABRIAC, P.-A. 2014. Mesure du comportement hygrothermique du pisé. <https://hal.science/tel-01413611/>.
- CHAUHAN, P., EL HAJJAR, A., PRIME, N., AND PLÉ, O. 2019. Unsaturated behavior of rammed earth: Experimentation towards numerical modelling. *Construction and Building Materials* 227, 116646.
- CHEHADE, S., SIDI-BOULENOUAR, R., DUJARDIN, N., ET AL. 2024. Experimental Investigation of Hygrothermal Properties of Raw Earth Compressed Blocks. *Second RILEM International Conference on Earthen Construction*, Springer Nature Switzerland, 428–437.
- CHITIMBO, T. 2023. Vulnérabilité des structures en pisé vis-à-vis des conditions hydriques. <https://www.theses.fr/s252435>.
- CHITIMBO, T., PRIME, N., PLE, O., AND ABDULSAMAD, F. 2022. Drying experiment on rammed earth structure. *European Journal of Environmental and Civil Engineering* 27, 1–17.
- COLINART, T., MCGREGOR, F., DUC, M., ET AL. 2024. Preliminary Results of Interlaboratory Tests on Hygrothermal Properties of CEB. *Second RILEM International Conference on Earthen Construction*, Springer Nature Switzerland, 458–465.
- FABBRI, A., MOREL, J.-C., AUBERT, J.-E., BUI, Q.-B., GALLIPOLI, D., AND REDDY, B.V.V., EDS. 2022. *Testing and Characterisation of Earth-based Building Materials and Elements: State-of-the-Art Report of the RILEM TC 274-TCE*. Springer International Publishing, Cham.
- FONTAINE, L. AND ANGER, R. 2009. *Bâtir en terre: du grain de sable à l'architecture*. Belin, Paris.
- GANDREAU, D. AND JOFFROY, T. 2013. Inventaire 2012 des biens en terre du patrimoine mondial. UNESCO, 228–231.
- GIADA, G., CAPONETTO, R., AND NOCERA, F. 2019. Hygrothermal Properties of Raw Earth Materials: A Literature Review. *Sustainability* 11, 19, 5342.
- GIUFFRIDA, G., IBOS, L., BOUDENNE, A., AND ALLAM, H. 2024. Exploring the integration of bio-based thermal insulations in compressed earth blocks walls. *Construction and Building Materials* 418, 135412.
- HEBERLE, É. 2013. *CEREMA : étude HYGROBA - Etude de la réhabilitation hygrothermique des parois anciennes*. .
- HOUBEN, H., GUILLAUD, H., AND CRATERRE. 1989. *Traité de la construction en terre*. .
- INDEKEU, M. 2023. L'impact de l'isolation intérieure sur les performances hygro-thermiques des murs en pisé. .
- LE TIEC, J.-M., MISSE, A., DAYRE, M., DOAT, P., AND JOFFROY, T. 2020. *Construire en pisé: prescriptions de dimensionnement et de mise en oeuvre*. Le Moniteur, Antony.
- LOSINI, A.E., WOLOSZYN, M., CHITIMBO, T., ET AL. 2023. Extended hygrothermal characterization of unstabilized rammed earth for modern construction. *Construction and Building Materials* 409, 133904.
- POUPARD, T., FABRE, F., POUILLAIN, P., ISSAADI, N., AND BONNET, S. 2024. Rammed Earth Building: Contribution of Moisture Transfer on Indoor Comfort. *Second RILEM International Conference on Earthen Construction - ICEC 2024*, Springer Nature Switzerland, 184–193.
- TERA, ARESO, ARPE NORMANDIE, ET AL. 2018. Guide de bonne pratique pisé de la construction en terre crue : pisé. .
- TESTING AND CHARACTERISATION OF EARTH-BASED BUILDING MATERIALS AND ELEMENTS: STATE-OF-THE-ART REPORT OF THE RILEM TC 274-TCE. 2022. .
- TOPP, G.C., DAVIS, J.L., AND ANNAN, A.P. 1980. Electromagnetic determination of soil water content: Measurements in coaxial transmission lines. *Water Resources Research* 16, 3, 574–582.
- VINCESLAS, T. 2019. Caractérisation d'éco-matériaux terre-chanvre en prenant en compte la variabilité des ressources disponibles localement.